ACTA STEREOL 1995; 14/1: 29-34
STERMAT'94
ORIGINAL SCIENTIFIC PAPER

QUANTITATIVE CHARACTERISATION OF WELD SIMULATED STRUCTURES IN DUPLEX STAINLESS STEEL SAF 2205

Jacek Komenda and *Rolf Sandström

Swedish Institute for Metals Research, Drottning Kristinas väg 48,
S-114 28 Stockholm, Sweden
*Professor in Applied Materials Technology, Royal Institute of Technology,
S-100 44 Stockholm, Sweden

ABSTRACT

Microstructures of SAF 2205 type steel after weld simulation were investigated using the automatic image analysis system. Conventional etching produced weak contrast between phases. After modification of the colour etching method, a clear distinction between the austenite and ferrite phases was obtained. Microstructure was quantitatively characterised by the area fraction and the width of austenite at ferrite grain boundaries, also by mean free distance between the austenite islands distributed in the ferrite matrix. The measured structural parameters are related to Charpy-V impact energy data. In particular the width of the austenite islands located at the ferrite grain boundaries had a significant influence on the impact energy.

Keywords: duplex stainless steels, image analysis, impact energy, weld simulation.

INTRODUCTION

Duplex stainless steels possess excellent corrosion resistance, good weldability and good mechanical properties. Modern duplex steels contain approximately the same amounts of ferrite and austenite. This ratio is also maintained in the base metal during welding; however in the heat affected zone (HAZ) the contents of austenite and ferrite depend on the weld thermal cycle. Increasing the austenite content of the weld metal improved tensile ductility and impact toughness (Sridhar et al., 1984). Austenite formation can be suppressed during the welding process resulting in higher ferrite content (Gretoft et al., 1988). Large ferrite grain size and low volume fraction of austenite led to lower impact toughness of the welded material (Enjo et al., 1988). Coarse ferrite grain gave a limited austenite reformation on cooling, with direct consequences for both mechanical properties and corrosion resistance (Ferreira and Hertzman, 1991). Since the relations between ferrite and austenite contents and morphologies are important for the mechanical properties and corrosion resistance of duplex steel weldment, the present paper aims to present a method to determine weld microstructures and to quantitatively characterise them using an automated image processing.

MATERIAL

Weld simulated specimens and impact energy data were used from the earlier work (Cao and Hertzman, 1991). Chemical compositions of steels and Swedish standard specification of SAF 2205 (SS 2377) are given in Table 1. The specimens were the half size Charpy V-notch blanks (5×10×60 mm) machined from the 7 mm plates with the long axes in the rolling direction. Weld simulation was performed on a resistance heated weld simulator with controlled temperature cycles and water cooling. HAZ was located in the centre of the specimen. Table 2 presents the thermal cycles of weld simulation and Charpy-V impact energy data. Specimens were divided into two groups. These with fast cooling rate, (F), were selected into group I. The ones with medium cooling rate, (M), and slow cooling rate, (S), were in group II. Quantitative metallographic examination was performed in HAZ.

Table 1. Chemical composition of steels (charge analysis, wt%) with SAF 2205 specification.

Steel	C	Si	Mn	P	S	Cr	Mo	Ni	N
No. 1	0.024	0.42	1.5	0.024	0.001	22.0	3.0	5.6	0.12
No. 2	0.021	0.40	1.5	0.024	0.001	22.0	3.2	5.7	0.18
No. 3	0.026	0.45	1.9	0.010	0.003	25.1	3.0	5.8	0.17
SS 2377 min.	-	-	-	-	-	21.0	2.5	4.5	0.10
max.	0.050	1.00	2.0	0.030	0.020	23.0	3.5	6.5	0.20

Table 2. Welding simulation thermal cycles and Charpy-V impact energy (tested at room temperature) of investigated specimens, (Cao and Hertzman, 1991).

Group number	Steel	Specimen	Holding time at 1350°C, [s]	Cooling rate, [°C/s]	Impact energy, [J]
I	No. 3	Cr/5/F	5	430	29
	No. 1	N/5/F	5	430	48.5
	No. 2	10/F	10	430	45
	No. 2	5/F	5	430	50
II	No. 2	10/S	10	160	76
	No. 2	10/M	10	300	84
	No. 2	5/S	5	160	89
	No. 2	5/M	5	300	65

ETCHING METHOD

The colour etching method using Beraha II solution (Weck and Leistner, 1983) was modified (Komenda, 1990) to ensure good contrast between ferrite and austenite. A set of three chemicals was prepared in separate vessels: a) 25 ml concentrated hydrochloric acid Hcl; b) 100 ml Beraha etchant that is a mixture of 100 ml Beraha II stock solution (Weck and Leistner, 1983) and 1 g of potassium metabisulphite $K_2S_2O_5$; c) 200 ml of solution: 3 g calcium hydroxide $Ca(OH)_2$ in 200 ml distilled water.

Because of high hydrofluoric acid content, the etchant b) was applied in a plastic vessel and plastic pliers were used to hold the specimen. After grinding, specimens were polished with 3 μm and 1 μm diamond paste and washed in alcohol. Then, without drying, the specimen was immersed in solution a) for 5 seconds, next in b) for 4 seconds and then in c) for 8 seconds. Finally, the specimen was washed in distilled water and then in alcohol. Since the etching was performed at several steps, the method was called stepwise etching.

IMAGE ANALYSIS

Microstructures were investigated using the image analysis system IBAS 2000 (Kontron GmbH/Zeiss, 1986). The area fraction and size of non-metallic inclusions were measured in all specimens. To characterise the content of austenite phase in the specimens of group I, the global area fraction, area fraction at ferrite grain boundaries and area fraction inside the ferrite grains were used. The size of austenite islands inside ferrite grains was measured as circle area equivalent diameter. The mean free distance (MFD) between them was measured according to the formula (Underwood, 1970):

$$MFD = (1-A_\gamma) / N_L \qquad (1)$$

A_γ refers to the global area fraction of austenite and N_L is the number of interceptions of austenite islands per unit length of test lines applied in 0°, 45°, 90° directions to the long axis of the specimen. The width of elongated austenite islands at ferrite grain boundaries was measured using two parameters. The average value of intercept length from the horizontal test lines represented random width of the austenite island, W_h. The second parameter, W_b , was obtained from the measurement of two distances perpendicular to each other, based on the areal moments of inertia (Kontron GmbH/Zeiss, 1986). For the ellipsoidal austenite island the size of major and minor axes were obtained. The minor axis size

was the width of an austenite island, W_b. Fig. 1 illustrates the measurement principles for W_h and W_b .

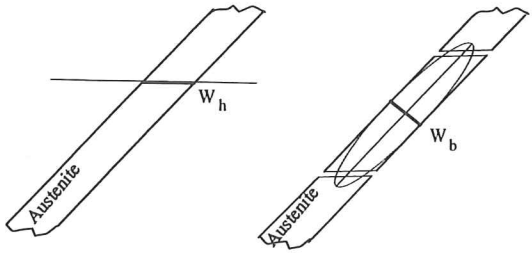

Fig. 1. The principles of the width measurement methods (W_h and W_b respectively) applied to the austenite phase located along the ferrite grain boundaries.

To measure W_b long austenite islands were cut into sections. It was achieved by subtraction of an image with horizontal lines from a binary image of the structure. The principles of image processing are shown in Fig. 2. The austenite in specimens of group II was characterised by the global area fraction, mean free distance (MFD) and circle area equivalent diameter. The last parameter was applied to the austenite agglomerates (here called packages), showing a Widmannstätten type structure.

RESULTS

No post-welding inclusions were present in the structure. Some amount of silicates and sulphides was measured: 0.13 vol% in Cr/5/F and N/5/F and from 0.05 to 0.07 vol% in the remaining specimens. The average size of inclusions was from 2.2 to 2.8 μm. Figs. 3a to 3h present examples of investigated microstructures. With decreasing cooling rates the austenite phase first nucleated at ferrite grain boundaries, next grew inside grains as needles and then austenite particles appeared inside ferrite grains. Widmannstätten type structures are shown in Figs. 3f and 3h. The largest ferrite grains (234 μm) were in 10/F specimen. Cr/5/F, N/5/F and 5/F had grains with a mean size of 153 μm, 203 μm and 159 μm respectively. Grains were equiaxed. Austenite area fraction, mean free distance, width of islands located at ferrite grain boundaries (W_h and W_b) and the size of austenite islands inside ferrite grains are given in Table 3. Table 4 presents austenite characteristics measured in specimens of group II. Under similar thermal cycles the lowest austenite content was measured in steels that contained more Cr and less N in comparison to the SAF 2205 specification. Slow cooling produced more austenite and the width of austenite at ferrite grain boundaries was larger. W_h and W_b parameters showed strong relation to each other with a regression coefficient 0.97 . Since the measurement of W_b is more time consuming, the W_h parameter was applied in further analysis. No effect of the ferrite grain size on Charpy-V impact energy tested at room temperature was found, although this was anticipated from the literature information (Enjo et al., 1988). The larger the ferrite grain size, the lower should the impact energy be but in the present work this effect was not observed. However, a clear relation with a correlation coefficient of 0.90 was noted between the austenite area fraction A_γ and impact energy C_V :

$$C_V = a + b \times A_\gamma \quad (2)$$

where a = 31 [J] and b = 1.9 [J/% austenite].

Even stronger correlation was found between the width of the austenite phase located at the ferrite grain boundaries and the impact energy. Fig. 4 presents this relation for the specimens of group I. The correlation coefficient was 0.97 and the following equation was obtained from the regression analysis:

$$C_V = a + b \times W_h \quad (3)$$

where a = 17.6 [J] and b = 7.8 [J/μm].

The relation between impact energy and the size of austenite particles inside ferrite grains showed a correlation coefficient value of 0.68 .

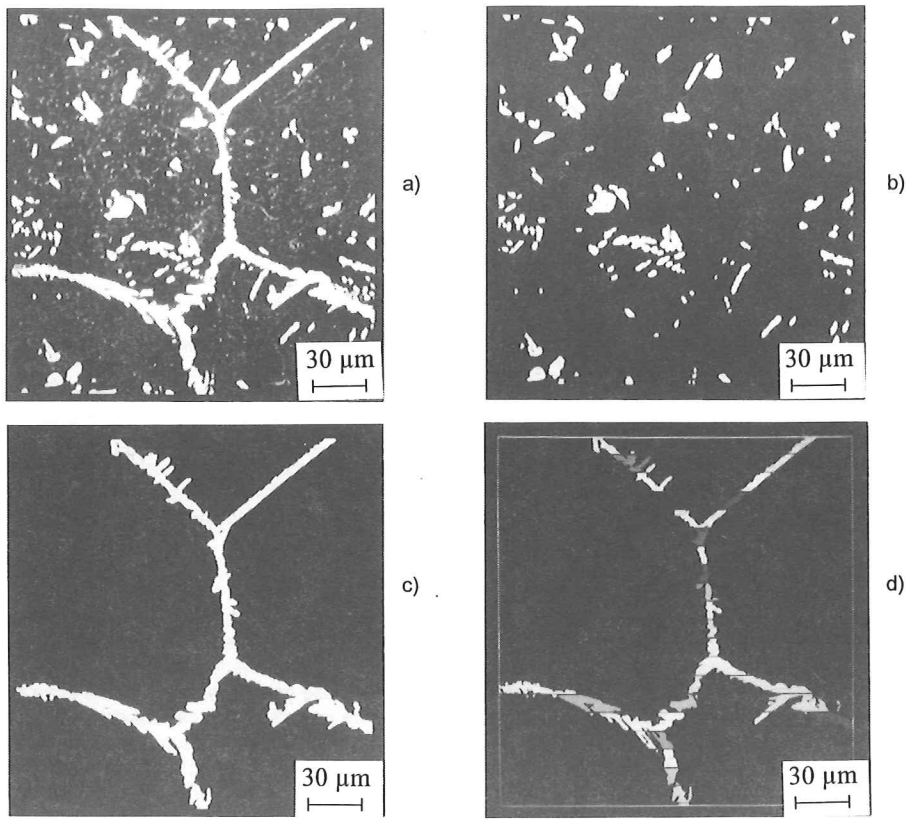

Fig. 2. Image processing steps for ferrite - austenite structure: a) original image, (etched structure), b) binary image of austenite inside ferrite grains, c) austenite at ferrite grain boundary, d) austenite at ferrite grain boundary cut by subtracted line pattern.

Table 3. Mean values of parameters measured on austenite phase in specimens of group I.

Specimen	Area fraction, %			Mean free distance µm	Width, W_h µm	Width, W_b µm	Island size inside grains µm
	global	at ferrite grain boundaries	inside grains				
Cr/5/F	1.0	0.8	0.2	152	1.5	1.6	2.5
N/5/F	3.7	2.1	1.6	67	3.6	3.2	3.3
10/F	10.9	3.5	7.4	24	3.9	4.2	4.2
5/F	12.5	5.9	6.6	21	4.1	4.0	3.4

DISCUSSION

The amount and distribution of the austenite phase was found to be the main factor controlling the impact energy of weld simulated specimens. A lower austenite content has been measured in specimens that contained less nitrogen and more chromium, respectively. The holding time at peak temperature during weld simulation did not affect the amount of austenite but the cooling rate did. With the lower cooling rate the specimens contained more austenite. The area fraction and size of inclusions varied in a too narrow range to show the effect on impact energy. Nor the results did not show any relation between ferrite grain size and impact energy. It was assumed due to a stronger influence of the auste-

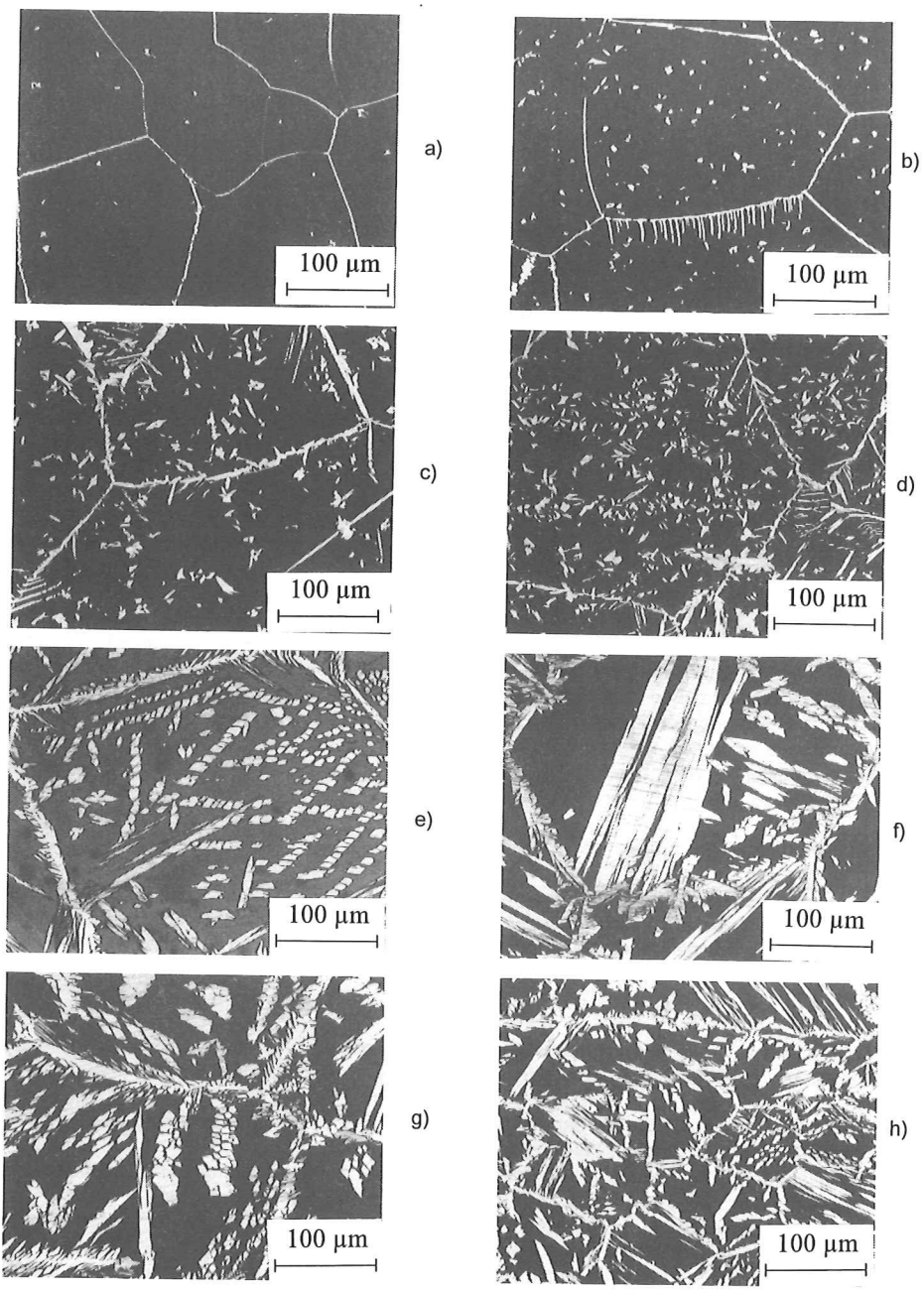

Fig. 3. Investigated microstructures of duplex stainless steel weldment (HAZ).
a) Cr/5/F, b) N/5/F, c) 10/F, d) 5/F, e) 10/S, f) 10/M, g) 5/S, h) 5/M.

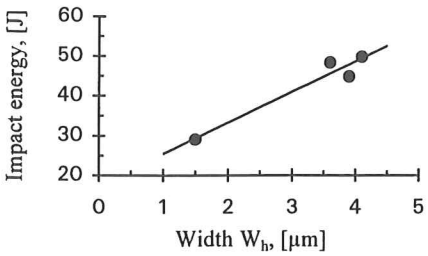

Fig. 4. Charpy-V impact energy versus width of austenite at ferrite grain boundaries.

Table 4. Mean values of parameters measured on austenite phase in specimens of group II.

Specimen	Area fraction %	Mean free distance μm	Package size μm
10/S	21.0	20	54
10/M	24.9	19	59
5/S	25.6	18	94
5/M	26.5	15	71

nite content and distribution on the impact properties. A very strong relation was found between the width of austenite located at ferrite grain boundaries and impact energy. The relation between the mean free distance of austenite islands and impact energy was not very much pronounced. An attempt to describe the austenite packages quantitatively in specimens of group II was made, where the IBAS system was applied in a semi-automatic way. However, the general measurements were performed in automatic way and the time of work was relatively short concerning the amount of information.

CONCLUSIONS

The etching method presented in the paper provides a clear distinction between austenite phase and ferrite matrix. In agreement to the literature information a pronounced correlation was observed between the austenite content and impact energy. The width of the austenite located at ferrite grain boundaries showed a relation to the Charpy-V impact energy of the weld simulated specimens. As the width of austenite increased, so did the impact energy. This relation was found to be stronger than the one between austenite content and impact energy, indicating that the austenite in ferrite grain boundaries plays a special role.

ACKNOWLEDGEMENTS

The project was performed within the General Research Programme at the Swedish Institute for Metals Research and the financial support is gratefully acknowledged. The authors thank Dr Staffan Hertzman, Swedish Institute for Metals Research, for supplying the specimens and impact test data.

REFERENCES

Cao HL, Hertzman S. The relationship between impact properties and welding simulated microstructures in three duplex stainless steels. In: Proc Int Conf Duplex Stainless Steels, Beaune France, 1991.

Enjo T, Kuroda T, Imanishi R. Microstructure and toughness in weld heat affected zone of duplex stainless steel. Transactions of JWRI 1988; 17/2: 105-111.

Fereira PJ, Hertzman S. δ-ferrite grain growth in simulated high temperature HAZ of three duplex stainless steels. In: Proc Int Conf Duplex Stainless Steels, Beaune France, 1991.

Gretoft B, Rigdal SL, Karlsson L, Svensson LE. Influence of welding process on mechanical properties of duplex stainless steel weld metals. In: Proc Conf Stainless Steels '87, Stockholm Sweden, 1988.

Komenda J. Quantitative characterization of weld simulated microstructures in the duplex stainless steel SAF 2205. Swedish Institute for Metals Research report IM-2581, 1990.

Kontron GmbH/Zeiss, IBAS - The Interactive Image Analysis System, Eching, Germany, 1986.

Sridhar N, Flasche LH, Kolts J. Corrosion and mechanical properties of duplex stainless steel weldments. In: Developments in stainless steel technology, Detroit, Metals Park, ASM, 1985: 341.

Underwood E. Quantitative Stereology. Addison-Wesley Publ Co , 1970: 82-83.

Weck E, Leistner E. Metallographic instruction for colour etching by immersion, Part II: Beraha colour etchants and their different variants. DVS, 1983.